Coordination and competition between soil magnetic particles driven by contrary climate development

Yunfeng Cai[1], Xiaoyong Long[1*], Xianqiang Meng[2], Junfeng Ji[3], Yong Wang[1], Shiyou Xie[1]

[1]School of Geographical Sciences, Southwest University, Chongqing, China

[2] State Key Laboratory of Lake Science and Environment, Nanjing Institute of Geography and Limnology, Chinese Academy of Sciences, Nanjing, China

[3]Institute of Surficial Geochemistry, College of Earth Sciences and Engineering, Nanjing University, Nanjing, China

*Corresponding author: Xiaoyong Long (longxy@126.com)

Key Points:

- Dry and warm climate favors the dehydration of amorphous iron oxides to form antiferromagnetic hematite and ferrimagnetic particles
- Wet and cool climate mainly produces goethite and leads to the competition between antiferromagnetic hematite and ferrimagnetic particles
- Temperature is as important as precipitation when reconstructing paleoclimate with strong dry-wet cycles and climate pattern shifts.

Abstract

The ferrimagnetic (FM) and antiferromagnetic (AFM) particles of iron oxides are considered pedogenic and climatic indicators due to their enrichment with comparable increasing in rainfall and temperature. However, the opposite changes in rainfall and temperature result in rapid change of relative humidity (RH), which could lead to their competition and transformation. We examined two soil sequences undergone contrary climate development on the eastern edge of the Tibetan Plateau. The dry and warm climate with low RH favors the coordinative enrichment of AFM hematite and FM particles, while the wet and cool climate with high RH mainly produces goethite but leads to competition between low content AFM hematite and FM particles. The outcome well interprets the changing relationship between color and magnetism in soils and sediments, and suggests that temperature is as important as precipitation in paleoclimate reconstruction based on iron oxides, especially during strong dry-wet cycles and climate pattern shifts.

Key words: Magnetism; Color; Iron oxides; Relative humidity; Paleoclimate reconstruction;

Plain Language Summary

Iron oxides are commonly enriched on the surface of Earth as the weathering products driven by comparable increasing of rainfall and temperature. The color and magnetism dominated by antiferromagnetic (AFM) and ferrimagnetic (FM) particles of iron oxides are considered sensitive pedogenic and climatic indicators. However, the contrary changes in rainfall and temperature often lead to remarkable change of relative

humidity (RH), which could promote their competition and transformation into iron hydroxides. The uplift of the Tibetan Plateau has led to different orographic elevation and contrary climate development on the eastern edge in Yunnan Plateau and Guizhou Plateau. We found that the present dry and warm climate in the Yunnan Plateau with low RH favors the dehydration of amorphous iron oxides to form AFM hematite and FM particles concomitantly, while the present wet and cool climate in the Guizhou Plateau with high RH mainly produces goethite and leads to the competition between the low content of AFM hematite and FM particles. This behavior explains changing relationship of magnetism and color in soils and sediments. It also suggests that temperature is as important as precipitation when reconstructing paleoclimate based on iron oxides, especially during strong dry-wet cycles and climate shifts.

1 Introduction

Iron oxides are ubiquitous on the surface of Earth and Mars [Christensen et al., 2001; Cornell and Schwertmann, 2003] and can be classified into antiferromagnetic (AFM) and ferrimagnetic (FM) particles according to magnetic properties [Cornell and Schwertmann, 2003; Liu et al., 2012a]. The former including hematite (Hm, α-Fe_2O_3) and goethite (Gt, α-FeOOH) predominate color [Cornell and Schwertmann, 2003; Long et al., 2016] while the latter including magnetite (Mgt, Fe_3O_4) and maghemite (Mgh, γ-Fe_2O_3) predominate magnetism in soils and sediments [Liu et al., 2012a]. These particles are commonly enriched as immobile weathering products under aerobic conditions with comparable increase in rainfall and temperature [Long et al., 2011, 2016; Torrent et al., 2006]. Consequently, color and magnetism are considered reasonable pedogenic and climatic indicators in soil taxonomy and paleoclimate reconstruction [Maher,1998; Mullins, 1977]. Over the past few decades, magnetic properties have been successfully incorporated into paleorainfall reconstruction, especially with aeolian sediments in the Chinese Loess Plateau (CLP) [Heller et al, 1991, 1993; Liu et al., 1995, 2003; Liu et al., 2007a; Maher, 2016; Nie et al., 2008, 2013] and other temperate regions [Chlachula, 2003; Liu et al., 2001, 2012b]. Meanwhile, color indices of soils have also been employed to reflect changes in temperature [Yang et al., 2001; Yang and Ding, 2003].

However, growing evidence has been accumulated on asynchronous changes of color indices and magnetic properties in soils across wide climate regimes [Gao et al., 2018; Han et al., 1996; Maher, 1998], as well as in the sediments recording Quaternary and Neogene climates, especially by paleosol layers such as S1 [Liu and Ding, 2003], S5 [Guo et al., 2013; Liu et al., 2006], and S9 [Xie et al., 2003] in Chinese Loess Plateau (CLP), or by red clay in North China [Balsam et al., 2004; Hao et al., 2009; Ji et al., 2004; Nie et al., 2014;] and South China [Han et al., 1996; Long et al., 2011] driven by strong dry-wet cycles and climate pattern shifts. Therefore, other soil chemical and mineral parameters have been introduced to understand these shifting correlations. The free iron (Fe_d) indicating the total amount of pedogenic iron oxides has been applied to trace the change of pedogenic intensity [Ding et al., 2001]. The amorphous iron (Fe_o) reflecting uncrystallized iron oxides was used to interpret the formation and transformation of FM particles [Hu et al., 2009b]. Moreover, the ratio of Hm and Gt [Ji et al., 2001] was introduced to reconstruct changes in the relative humidity (RH) rather than individual changes in rainfall and temperature [Balsam, 2004; Hao et al., 2009; Ji et al., 2001, 2004;]. These sediment layers are often characterized by high pedogenic intensity [Ding et al., 2002], lower iron oxide crystallinity [Hu et al., 2009a] and significant changes in Hm/Gt under warmer stages [Ji et al., 2004].

Theoretically, AFM Hm forms under warm, dry and seasonal climates, while Gt forms under cool, wet and less seasonal climates [Long et al.,2016; Schwertmann, 1985;], which is consistent with the aging experiment of amorphous iron oxides under different RH [Torrent et al., 1982]. Moreover, the formation of FM Mgh particles with differing sizes competes with formation of AFM Hm as an intermediate product from amorphous iron oxide under aerobic conditions [Barrón and Torrent, 2002; Torrent et al., 2006], which also depends on the formation efficiency of the Hm estimated by Hm/(Hm+Gt) [Long et al., 2011, 2015]. Pedogenesis in aeolian sediments, however, is also influenced by the dust provenance [Li et al., 2009], deposition rates [Kukla, 1987] and erosion processes [Lu et al., 2006] besides climate-controlled chemical weathering. Therefore, it is difficult to discern the independent contributions of climate to the formation of pedogenic iron oxides and related changes in color and magnetism.

The Yunnan Plateau (YP) and the Guizhou Plateau (GP) on the eastern edge of the Tibetan Plateau (TP) have undergone differential uplifts and contrary climate development at least since the Quaternary [Yang et al., 2010; Yan et al., 2011]. As a result, marked soil reddening in the YP with low RH and soil yellowing in the GP with high RH have been observed. These conditions provide a good opportunity to investigate and understand the relationship between different magnetic particles driven by strong dry-wet cycles or climate pattern shifts.

2 Materials and Methods

2.1 Geographical settings and soil sampling

The YP and GP belong to the tectonic extrusion zone of the TP [Molnar and Tapponnier, 1975]. Compared with the flat surface of TP with an average altitude of approximately 4000 m, the surfaces of the YP and GP are rugged with an average altitude of approximately 2000 m and 1100 m, respectively [Zhao et al., 2015] **(Appendix A)**. We collected two saprolitic soil profile sequences from the YP and GP underlain by the widespread Triassic carbonate rocks [Feng, 2005]. The profiles of YP1, YP2 and YP3 were collected from the YP under increasing mean annual temperature (MAT) from 13.4 °C to 18.2 °C and decreasing mean annual precipitation (MAP) from 924 mm/yr to 762 mm/yr. Similarly, the profiles of GP1, GP2 and GP3 were collected under increasing MAT from 12.9 °C to 14.4 °C and decreasing MAP from 937 mm/yr to 899 mm/yr. The MAT and MAP are close to the southmost of CLP [Jiao and Liu, 1984]. Since the RH is defined as the ratio of the actual water vapor pressure to the saturation vapor pressure, the increase temperature often increases the saturation vapor pressure but the decreasing precipitation often decreases the actual water vapor pressure [Pelxoto et al., 1996]. The opposite change trends in MAT and MAP enlarge the difference of RH between YP from 58% to 73%, and GP from 79% to 82% on the GP [Xu, 1991], which almost covers the range of RH from 50% to 70 % in present CLP as well as the range of 70 to 80% in East China [Jiao and Liu, 1984], where the loess and red clay are widely deposited [Hu et al., 2009a; Liu, 1985]. Moreover, the RH is around the climatic threshold that controls soil reddening and yellowing, as proposed in our previous studies [Long et al., 2016]. As a result, the saprolitic soils on the YP have demonstrated a common reddening trend (3.2 YR-6.3 YR) while the soils on the GP have demonstrated a significant yellowing trend (6.2 YR-9.6 YR). These profiles were sampled on the local highland and were covered by natural vegetation ranging from herbaceous plants in YP to evergreen forests in GP. The soil type in the YP can be categorized as an Acrisol, while that in the GP can be categorized as an Alisol [IUSS Working Group WRB, 2015]. The soil samples were collected from the surface to the bottom of the outcrops at intervals of 20 cm or 40 cm covering the main horizons depending on the thickness of the outcrops.

2.2 Chemical and physical measurement

The air-dried samples were sieved using a 2 mm sieve and ground into powder for chemical analysis. The total iron (Fe_t) was determined with an ARL9800XP + X-ray spectrophotometer. Free iron (Fe_d) and amorphous iron (Fe_o), which reflects the total pedogenic iron oxides and amorphous iron oxides, were extracted by the citrate-bicarbonate-dithionite (CBD) method [Mehra and Jackson, 1958] and ammonium oxalate method [Schwertmann, 1964], respectively. Diffuse reflectance spectra (DRS) were measured with a Perkin Elmer Lambda 900 UV/VIS/NIR spectrometer at 2 nm intervals. The standard Hm and Gt minerals used in the experiment were the Pfizer

R1599 pure red from Pfizer Company and Synox HY610 pure yellow nanoscale iron oxides from the Hoover Color Corporation. The redness was calculated according to the ratio of mean reflectance between the red-light band (630 ~ 700 nm) and the visible light band (400 ~ 700 nm) [Judd and Wyszecki, 1975]. The Hm content was estimated using a working curve established by the sample substrate after CBD treatment mixed with a series of standard Hm and Gt samples in different ratios. Finally, the contents of Hm and Gt were calculated by the following equation when Fe_d is assigned to be the combination of Fe in stoichiometric Hm, Gt and Fe_o [Torrent et al., 2007, Long et al., 2011, Guo et al.,2021].

$$\text{Hm (g kg}^{-1}) = 0.0012\times e^{\,0.227 \times \text{Redness}}$$

$$\text{Gt (g kg}^{-1}) = 1.59 \times (Fe_d - Fe_o - Hm/1.43)$$

The magnetic susceptibility of all samples was measured in the laboratory at 0.47 kHz (χ_{lf}) and 4.7 kHz (χ_{hf}) with a Bartington MS2B susceptibility meter. The frequency-dependent magnetic susceptibilities χ_{fd} and $\chi_{fd}\%$ representing the absolute and relative contributions of superparamagnetic particles (SP) were calculated as $\chi_{lf} - \chi_{hf}$ and $(\chi_{lf} - \chi_{hf})/\chi_{lf} \times 100\%$, respectively [Dearing et al., 1996; Worm, 1998]. Meanwhile, anhysteretic remanent magnetization (ARM) indicating the content of single domain particles (SD) was imparted using a peak of the 100 mT alternating field and a 0.05 mT biasing field with a Molspin demagnetizer [Dunlop and Özdemir,1997]. The χ_{ARM} parameter was calculated from the ARM and normalized by the biasing field. Saturation isothermal remanent magnetization (SIRM) mostly reflecting coarser FM particles [Dunlop and Özdemir,1997] was attained at 1 T with the ASC-10 impulse magnetizer, and all the remanent magnetizations were measured in the AGICO JR6 spinner magnetometer. HIRM was calculated by (IRM_{-300mT} + SIRM)/2, which reflects the content of high-coercivity minerals, such as Hm or Gt [Liu et al., 2007b; Nie et al., 2010; Thompson and Oldfield, 1986;], and the *S-ratio* is calculated by –IRM_{-300mT}/SIRM, which indicates the relative abundance of FM to AFM particles [Thompson and Oldfield, 1986].

3. Results

As illustrated in **Figure 1**, the change of Fe_d/Fe_t is comparable in both sequences while the Hm/(Hm+Gt) demonstrates a significant shift from 0.20 to 0.98 in the profiles of YP sequence but remains low from 0.05 to 0.19 in the profiles of GP sequence **(Figure 1a)**. Correspondingly, the changes of Fe_d and Fe_o are also similar in both sequences **(Figure 1b)**, but the Hm content is much higher in the YP sequence while the Gt content is a little higher in the GP sequence **(Figure 1c)**. In addition, χ_{lf} ranges from 573.9×10^{-8} m^3 kg^{-1} to 4005.1×10^{-8} m^3 kg^{-1} in the YP sequence, which is much higher than that ranging from 8.7×10^{-8} m^3 kg^{-1} to 310.5×10^{-8} m^3 kg^{-1} in the GP sequence **(Figure 1d)**. More importantly, χ_{lf} changes in phase with redness in the YP sequence but out of phase in the GP sequence **(Figure 1d)**. The magnetic parameters χ_{fd}, χ_{ARM} and SIRM exhibit synchronous changes with χ_{lf} (**Figure 2a-2c**) except for HIRM **(Figure 2d)**.

4. Discussion

4.1 Comparable chemical weathering and significant iron oxides transformation driven by contrary climate development

Theoretically, the synchronous increasing of rainfall and temperature favors chemical weathering and the enrichment of iron oxides effectively because primary iron-bearing minerals are often preferentially weathered to form secondary iron oxides [Kump et al., 2000]. Under the wet and cool climate like the GP, high rainfall could enhance the chemical leaching, but chemical reaction rates would be retarded by lowered temperatures [Kump et al., 2000; White and Blum, 1995]. However, high RH favors the transformation of iron oxides into hydroxides such as Gt [Schwertmann, 1971]. Under the dry and warm climate like the YP, lower rainfall superimposed by the increased evaporation retards chemical leaching but the low RH promotes the dehydration of amorphous iron oxides to form iron oxides like Hm and Mgh [Barrón and Torrent, 2002; Grogan et al., 2003; Schwertmann, 1971]. The phenomena can be widely observed in mountainous regions [Long et al., 2016]. The RH around 73 ~ 79% controlling the contrast formation efficiency of Hm and FM particles between YP and GP in subtropical regions is lower than 80% observed in our previous studies in tropical regions [Long et al., 2016]. It verifies that the inflection point of RH often increases with temperature in laboratory experiments [Torrent et al., 1982].

4.2 Coordination and competition between FM particles and AFM Hm driven by contrary climate development

Since the pedogenic FM particles with differing sizes are considered intermediate products of Hm aging from amorphous iron oxides [Barrón and Torrent, 2002], the magnetic parameters are plotted versus Fe_o and Hm to explore their changing relationship **(Figure 3e-3h).** The magnetic parameters χ_{fd}, ARM, SIRM reflecting the amount of FM particles with increasing size reveal consistently positive correlation with similar Fe_o in both sequences (**Figure 3a-3c**) except for the HIRM mainly controlled by AFM Hm (**Figure 3d**). In contrast, the contents of FM particles and Hm are both much higher in the YP sequence than those in the GP sequence, but they change in phase in the YP sequence and out of phase in the GP sequence **(Figure 3e-3g)** except that the HIRM demonstrates more consistent correlation with Hm in both sequences **(Figure 3h)**. Moreover, in the YP sequence, $\chi_{fd\%}$, χ_{fd}/χ_{ARM}, ARM/SIRM, which indicate the ratio of fine FM particles to coarser FM particles**,** decrease significantly with Hm **(Figure 3i-3k)** but *S-ratio* keeps close to 1 **(Figure 3l)**. In the GP sequence, these parameters exhibit no significant trend with Hm **(Figure 3i-3k)** but the *S-ratios* demonstrate significant decrease with Hm **(Figure 3l)**.

These observations verify the genetic relationship between different FM particles and AFM Hm [Barrón and Torrent, 2002]. In natural systems, the amorphous iron could regulate the supply of precursors that forming FM particles while the crystallization of Hm controls the accumulation of FM particles [Hu et al., 2009b; Ren et al., 2020]. However, the correlation between FM particles and Hm depends on the formation efficiency of Hm controlled by RH [Long et al., 2015; Torrent et al., 2006]. The coordinative relationship between Hm and FM particles as revealed in the YP reddening soils under low RH, occurs under the condition with a high formation efficiency of Hm, indicate by Hm/(Hm+Gt) from 0.20 to 0.98. Under this condition, a large amount of FM particles including SP and SD particles has accumulated concomitantly, which allows grain growth of FM particles to transform into more stable AFM Hm [Navrotsky et al., 2008]. However, the formation of FM particles and AFM Hm has reached a dynamic equilibrium as indicated by stable *S-ratio* close to 1 with the increase of Hm. This process is consistent with the result revealed in aerobic soils with high Hm/(Hm+Gt) [Torrent et al., 2006], especially in the red Ferralsols with Hm/(Hm+Gt) above 0.6 [Long et al., 2015]. By contrast, the competitive relationship between Hm and FM particles, as revealed in the GP yellowing soils under high RH, occurs under the conditions with a low Hm/(Hm+Gt) from 0.05 to 0.19. Under this condition, the formation of iron oxides including FM particles and Hm, relative to iron hydroxides like Gt, are both inhibited [Tardy and Nahon, 1985; Trolard and Tardy, 1987]. However, due to the fluctuation of water activity in soils, there could be a competitive relationship between the limited contents of Hm and FM particles, which is indicated by the rapid decreasing of *S-ratio* with the increase of Hm. The competition can be observed in each profiles and whole sequences of the GP **(Figure 1c-1d).** It also accords with the yellow soils derived from the downslope of a subtropical granitic toposequence, with Hm/(Hm+Gt) < 0.2 and Hm% <1% [Guo et al., 2021]. Considering the competition is not accompanied by the systematic change in the grain size of FM particles (**Figure 3i-**

3k), the limited FM particles could transform or recrystallize from previously formed Hm due to higher thermodynamic stability of Mgh than Hm at the nanoscale [Navrotsky et al., 2008], especially when the content of Mgh particle is too low to grow in size [Jiang et al., 2018]. Actually, the changing content of FM particle estimated by χ_{lf} (8.7 ~ 310.5×10^{-8} m^3 kg^{-1}) in GP profiles roughly matches the Hm content changes (2.7~10.2 g/kg) if χ_{lf} of pure FM particles is estimated at around 110,000×10^{-8} m^3 kg^{-1} [Worm and Jackson, 1999]. The seesaw effect controlling the content of two iron oxide phases can also been found in yellow granitic soils [Guo et al., 2021].

4.3 Reconstructing strong dry-wet cycles and climate pattern shifts

The YP and GP sequences under contrast RH resulting from inverse change rainfall and temperature can help understand the formation and transformation of iron oxides undergone strong dry-wet cycles and climate shifts. However, the changes of rainfall and temperature are often considered comparable recorded by aeolian sediments, especially in East Asian monsoon regions [Kukla, 1987; Liu et al., 2012b; Maher, 2016]. As a result, there is often remarkable change in Fe_d or Fe_d/Fe_t controlled by chemical weathering but limited change in Hm/(Hm+Gt) controlled by RH in aeolian sediments [Balsam et al., 2004; Ding et al., 2001]. The Fe_d/Fe_t of the paleosols is often two times that of loesses [Ding et al., 2001], while the Hm/(Hm+Gt) is slightly lower in paleosols [Ji et al., 2004]. Correspondingly, the Hm and coexisting FM particles estimated by the product of Fe_d and Hm/(Hm+Gt) [Long et al., 2016] often change in phase with chemical weathering intensity, which makes magnetism and color reasonable pedogenic and climatic indicators. However, if the change of rainfall cannot keep in phase or even out of phase with temperature, the change of RH would result in the significant change of Hm/(Hm+Gt) which would cause incomparable change of magnetism and color, especially for the magnetic susceptibility and redness mainly controlled by fine FM particles and AFM Hm.

Actually, the magnetic susceptibility and redness are often coupled in loess depositing under dry and cool climates [Ji et al.,2004], but they are frequently observed as decoupled in paleosols forming under warm and wet climate like S1 [Liu and Ding, 2003], S5 [Guo et al., 2013; Liu et al., 2006], S9 [Xie et al., 2003] with Hm/(Hm+Gt) commonly decreasing below 0.2 [Hao et al., 2009]. These positive and negative relationships between Hm and FM particles in sediment sequences can be well compared with the YP and GP soil sequences. However, in the red clay with the Hm/(Hm+Gt) increasing up to 0.6 [Hao et al., 2009] undergone strong climate pattern shifts [Nie et al., 2008], uncertain and even opposite correlation between redness and magnetism were also found [Ding et al., 2001; Hu et al., 2009a; Nie et al., 2008;]. In the YP sequence as well as red Ferrosols with high Hm/(Hm+Gt), the positive correlation between FM particles and Hm still keeps although the formation rates of fine FM particles are observed to decrease with Hm [Long et al., 2015]. Therefore, the opposite correlation between redness and magnetism in the red clay in North and South China could also correlate with the increased iron crystallinity [Hu et al., 2009b], longer aging time [Jiang et al., 2018], less ligand protection [Ren et al., 2020] and warmer climate [Nie et al., 2008] to favor more rapid grain growth of FM particles and transformation into Hm.

It should be mentioned that the change of MAP from 762 mm/yr to 963 mm/yr is relatively limited from YP to GP while the change of MAT from 18.2℃ to 12.9℃ is significant. It suggests that the increasing temperature could also lead to strong soil reddening and magnetic enhancement via the dehydration of previous formed iron hydroxides even when the increasing of rainfall is limited. Moreover, although the soil redness and magnetism are commonly higher in the dry YP than those in the wet GP, the soil redness is commonly elevated with the increasing temperature in both sequences while the magnetism decrease with RH in dry YP but increases with RH in wet GP. The Hm content is more stable as a temperature indicator than FM particles as a precipitation indicator in wide range of climate. Consequently, it should be potential to use combined parameters to integrate AFM and FM particles in paleoclimate reconstruction based on iron oxides [Luo et al., 2021; Nie et al., 2017;], especially during strong dry-wet cycles and climate pattern shifts.

5. Conclusion

To unravel the changing relationship between AFM and FM particles and their climatic implications, we have examined two soil sequences under contrast RH in the YP and GP on the eastern edge of TP. The changes of total amount of iron oxides controlled by chemical weathering are comparable in both sequences. However, the AFM Hm and FM particles are much more enriched in the YP under low RH than in the GP under high RH. The dry and warm climate favors the dehydration of amorphous iron oxides to build up higher contents of AFM Hm and FM particles, while the wet and cool climate mainly produces goethite and leads to competition between Hm and FM particles. This outcome well interprets the synchronous and asynchronous changes in color and magnetism in soils and sediments, and also suggests that temperature is as important as precipitation in paleoclimate reconstruction based on iron oxides, especially during strong dry-wet cycles and climate pattern shifts under warm climate.

Acknowledgments

We thank Dr Ren Juan and Xing Dengchun for their help during the laborious field work in Southwest China. This study was co-supported by the National Natural Science Foundation of China (41877369) and the Natural Science Foundation of Chongqing, China (CSTC2018JCYJAX0456). The original data presented in this paper can be accessed through the public domain repository Zenodo at http://doi.org/10.5281/zenodo.4495880

Appendix A: **(a)** Sampling locations in the Yunnan Plateau (YP) and Guizhou Plateau (GP) on the east edge of the Tibetan Plateau (TP); **(b)** The YP is characterized by higher altitude and lower relative humidity (RH) than the GP. The profiles of YP1, YP2, YP3 and GP1, GP2, GP3 with increasing relative humidity were sampled in the YP and GP, respectively.

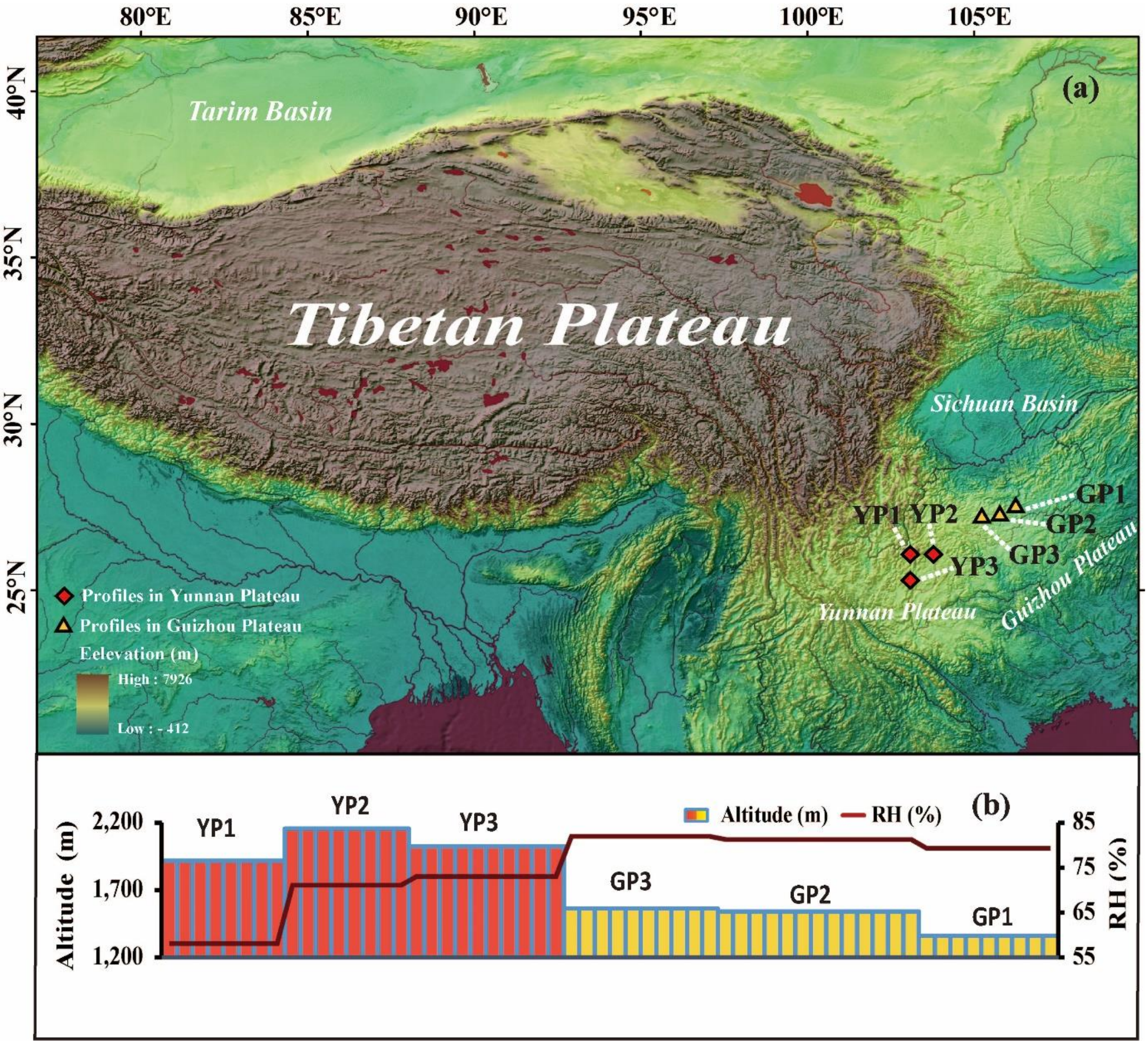

Figure 1. The Fe_d/Fe_t keeps comparable in both sequences but the Hm/(Hm+Gt) controlled by RH is much higher in the YP sequence than that in the GP sequence **(a)**. The ranges of Fe_d and Fe_o are also similar in both sequences **(b)** while the Hm is significantly higher in the YP sequence and the Gt is a little higher in GP sequence **(c)**. The magnetic susceptibility (χ_{lf}) changes in phase with the redness in the YP sequence but out of phase in the GP sequence **(d)**.

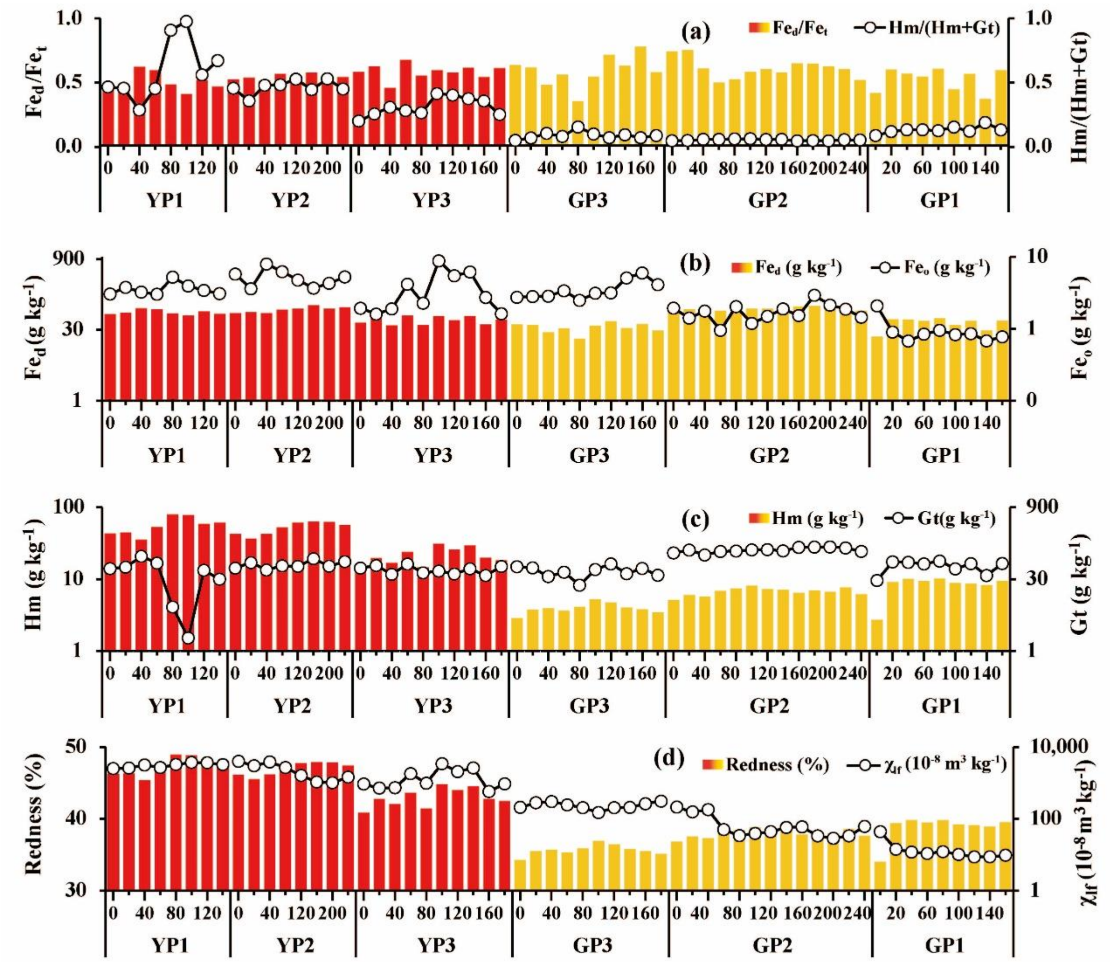

Figure 2. The magnetic parameters χ_{fd}, χ_{ARM}, SIRM are commonly higher in the YP sequence than the GP sequence and change consistently with the increase of χ_{lf} in both sequences **(a-c)** except for the HIRM **(d).**

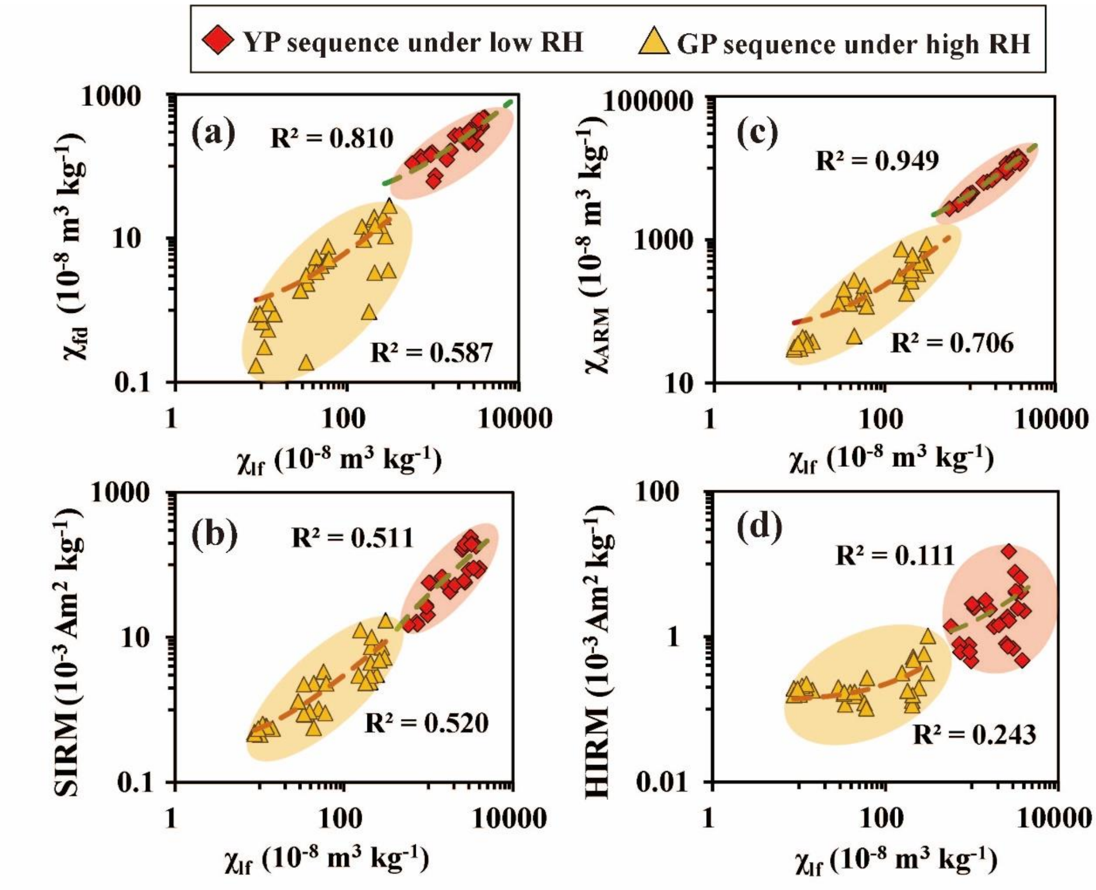

Figure 3. The magnetic parameters χ_{fd}, ARM, SIRM generally increase with Fe_o **(a-c)** except for HIRM **(d)**. Both the FM particles and Hm are more enriched and change in phase in the YP sequence, while they are less enriched and change out of phase in GP sequence (**e-g**) except that the HIRM demonstrates more consistent correlation with Hm in both sequences **(h)**. In the YP sequence, the magnetic parameters $\chi_{fd\%}$, χ_{fd}/χ_{ARM}, ARM/SIRM decrease significantly with Hm **(i-k)** but *S-ratio* keeps close to 1 (l). However, in the GP sequence, these ratio parameters exhibit no significant trend with Hm **(i-k)** but the *S-ratio* demonstrates significant decrease with Hm (**l**).

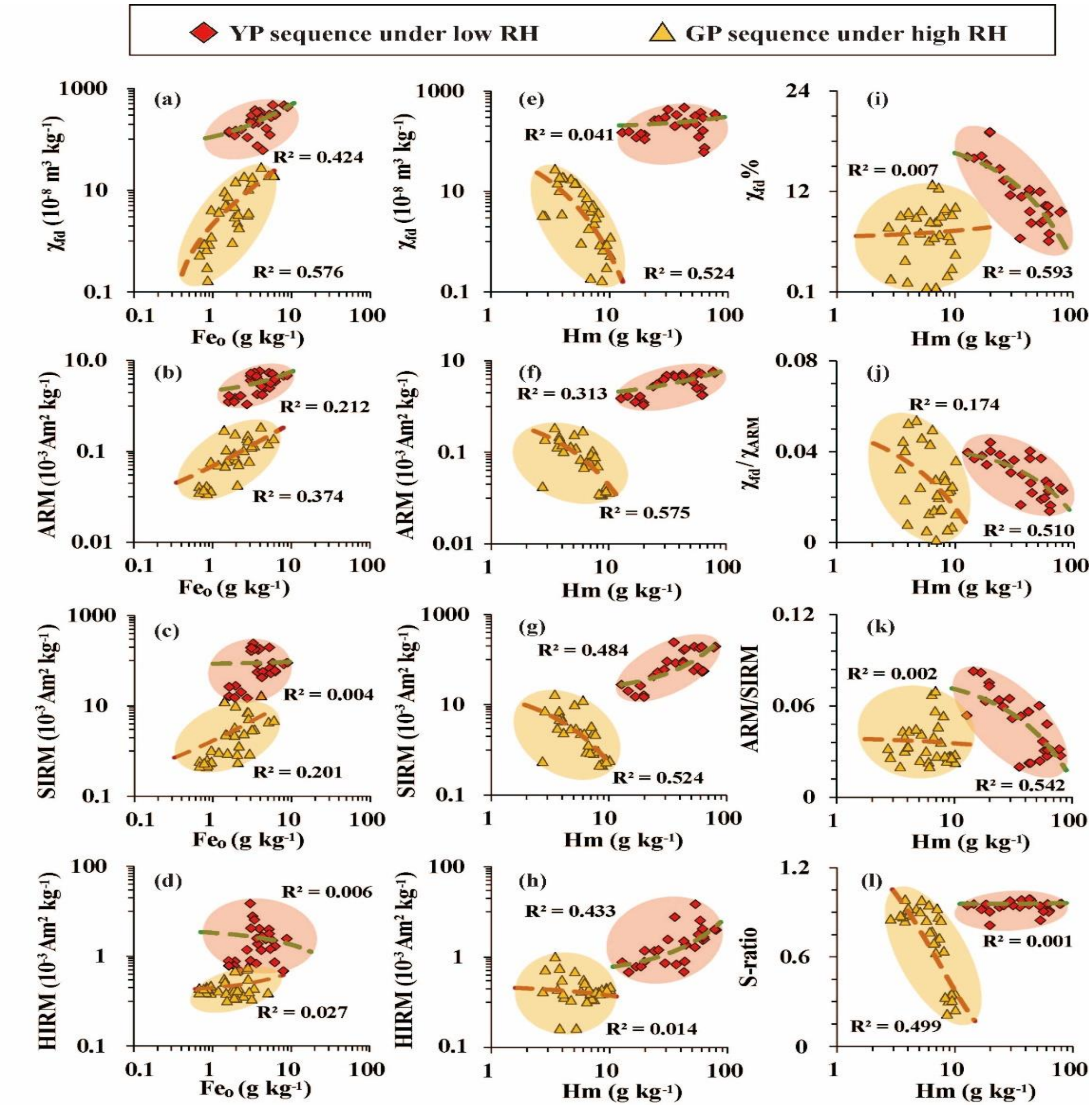

References

Barrón, V., and Torrent, J. (2002). Evidence for a simple pathway to maghemite in Earth and Mars soils. *Geochimica et Cosmochimica Acta*, **66**(15), 2801-2806. https://doi.org/10.1016/S0016-7037(02)00876-1

Balsam, W., Ji, J. F., and Chen, J. (2004). Climatic interpretation of the Luochuan and Lingtai loess sections, China, based on changing iron oxide mineralogy and magnetic susceptibility. *Earth and Planetary Science Letters*, **223**(3-4), 335-348. https://doi.org/10.1016/j.epsl.2004.04.023

Chlachula, J. (2003). The Siberian loess record and its significance for reconstruction of Pleistocene climate in north-Central Asia. *Quaternary Science Reviews*, **22**(18-19), 1879-1906. https://doi.org/10.1016/S0277-3791(03)00182-3

Christensen, P. R., Morris, R. V., Lane, M. D., Bandfield, J. L., and Malin, M. C. (2001). Global mapping of Martian hematite mineral deposits: Remnants of water-driven processes on early Mars. *Journal of Geophysical Research Planets*, **106**(E10), 23873-23886. https://doi.org/10.1029/2000JE001415

Cornell, R. M., and Schwertmann, U. (2003). The Iron Oxides: Structure, properties, reactions, occurrences and uses. (p435-437). Weinheim: Wiley-VCH Verlag GmbH & Co. KGaA.

Dearing, J. A., Dann, R. J. L., Hay, K., Less, J. A., Loverland, P. J., Maher, B. A., and O'Grady, K. (1996). Frequency-dependent susceptibility measurements of environmental materials. *Geophysical Journal International*, **124**, 228–240. https://doi.org/10.1111/j.1365-246X.1996.tb06366.x

Ding, Z. L., Yang, S., Sun, J., and Liu, T. (2001). Iron geochemistry of loess and red clay deposits in the Chinese Loess Plateau and implications for long-term Asian monsoon evolution in the last 7.0 Ma. *Earth and Planetary Science Letters*, **185**(1-2), 99-109. https://doi.org/10.1016/S0012-821X(00)00366-6

Ding, Z. L., Ranov, V., Yang, S. L., Finaev, A., Han, J. M., and Wang, G. A. (2002). The loess record in southern Tajikistan and correlation with Chinese loess. *Earth and Planetary Science Letters*, **200**(3-4), 387-400. https://doi.org/10.1016/S0012-821X(02)00637-4

Dunlop, D. J., and Özdemir, Ö. (1997). Rock Magnetism Fundamentals and frontiers. Cambridge Studies in Magnetism Series, xxi + 573 pp. Cambridge, New York, Port Chester, Melbourne, Sydney: Cambridge University Press.

Feng, J. L. (2005). Provenance of Terra Rossa on the carbonate rocks in Yunnan-Guizhou Plateau, China. Institute of Geographic Science and Natural Resources Research, CAS. https://ir.igsnrr.ac.cn/handle/311030/368

Gao, X. B., Hao, Q. Z., Wang, L., Oldfield, F., Bloemendal, J., Deng, C. L., Song, Y., Ge, J. Y., Wu, H. B., Li, F. J., Han, L., Fu, Y., and Guo, Z. T. (2018). The different climatic response of pedogenic hematite and ferrimagnetic minerals: Evidence from particle-sized modern soils over the Chinese Loess Plateau. *Quaternary Science Reviews*, **179**, 69-86. https://doi.org/10.1016/j.quascirev.2017.11.011

Grogan, K. L., Gilkesl, R. J., and Lottermoser, B. G. (2003). Maghemite Formation in

Burnt Plant Litter at East Trinity, North Queensland, Australia. *Clays and Clay Minerals*, **51**(4), 390-396. https://doi.org/doi: 10.1346/CCMN.2003.0510404

Guo, S. L., Cai, Y. F., Ren, J., Guan, Y. X., Xin, D. C., and Long, X. Y. (2021). Formation and migration of magnetic particles associated with iron oxide transformation at a hillslope scale. *Catena*, **197**(8)*, 104944*. https://doi.org/10.1016/j.catena.2020.104944

Guo, X. L., Liu, X. M., Li, P. Y., Lü, B., Guo, H., Qu, C., Liu, Z., and Ma, M. M. (2013). The magnetic mechanism of paleosol S5 in the Baoji section of the southern Chinese Loess Plateau. *Quaternary International*, **306**, 129-136. https://doi.org/10.1016/j.quaint.2013.02.033

Han, J. M., Lü, H. Y., Wu, N. Q., and Guo, Z.T. (1996). The magnetic susceptibility of modern soils in China and its use for paleoclimate reconstruction. *Studia Geophysica et Geodaetica*, **40**, 262–275. https://doi.org/10.1007/BF02300742

Hao, Q. Z., Oldfield, F., Bloemendal, J., Torrent, J., and Guo, Z. T. (2009). The record of changing hematite and goethite accumulation over the past 22 Myr on the Chinese Loess Plateau from magnetic measurements and diffuse reflectance spectroscopy. *Journal of Geophysical Research*, **114**(B12), 465-484. https://doi.org/ 10.1029/2009JB006604.

Heller, F., Liu, X. M., Liu, T. S., and Xu, T. C. (1991). Magnetic susceptibility of loess in China. *Earth and Planetary Science Letters*, **103**(1), 301-310. https://doi.org/10.1016/0012-821X(91)90168-H

Heller, F., Shen, C., Beer, J., Liu, X., Liu, T., Bronger, A., Suter, M., and Bonani, G., (1993). Quantitative estimates of pedogenic ferromagnetic mineral formation in Chinese loess and palaeoclimatic implications. *Earth and Planetary Science Letters,* **114**(2-3), 385-390. https://doi.org/10.1016/0012-821X(93)90038-B

Hu, X. F., Wei, J., Xu, L. F., Zhang, G. L., and Zhang, W. G. (2009a). Magnetic susceptibility of the Quaternary red clay in subtropical China and its paleoenvironmental implications. *Palaeogeography, Palaeoclimatology, Palaeoecology,* **279**(3-4), 216-232. https://doi.org/10.1016/j.palaeo.2009.05.016

Hu, X. F., Xu, L. F., Pan, Y., and Shen, M. N. (2009b). Influence of the aging of Fe oxides on the decline of magnetic susceptibility of the Tertiary red clay in the Chinese Loess Plateau. *Quaternary International*, **209**(1-2), 22-30. https://doi.org/10.1016/j.quaint.2009.02.019

IUSS Working Group WRB (2015). World reference base for soil resources 2014, update 2015, International soil classification system for naming soils and creating legends for soil maps. (p.144-146). World Soil Resources Reports 106, Food and Agriculture Organization of the United Nations, FAO, Rome.

Ji, J. F., Balsam, W., and Chen, J. (2001). Mineralogic and climatic interpretations of the Luochuan loess section (China) based on diffuse reflectance spectrophotometry. *Quaternary Research*, **56**(1), 23-30. https://doi.org/10.1006/qres.2001.2238

Ji, J. F., Chen, J., Balsam, W., Lu, H. Y., Sun, Y. B., and Xu, H. F. (2004). High resolution hematite/goethite records from Chinese loess sequences for the last glacial-interglacial cycle: rapid climatic response of the East Asian Monsoon to the tropical Pacific. *Geophysical Research Letters*, **31**(3), L03207. https://doi.org/ 10.1029/2003GL018975

Jiang, Z. X., Liu, Q.S., Roberts, A. P., Barrón, V., Torrent, J., and Zhang, Q. (2018). A new model for transformation of ferrihydrite to hematite in soils and sediments. *Geology*, **46**(11), 987-990. https://doi.org/10.1130/G45386.1

Jiao, B, C., Liu, M. G. (1984). Atlas of Physical Geography in China. (p.59-64). Beijing: SinoMaps Press.

Judd, D. B., and Wyszecki, G. (1975). Color in Business, Science, and Industry. (p.553). New York: John Wiley.

Kukla, G. (1987). Loess stratigraphy in central China. *Quaternary Science Reviews*, **6**(3-4), 209-219. https://doi.org/10.1016/0277-3791(87)90004-7

Kump, L. R., Brantley, S. L., and Arthur, M. A. (2000). Chemical weathering, atmospheric CO_2, and climate. *Annual Review of Earth and Planetary Sciences,* **28** (1), 611-667. https://doi.org/10.1146/annurev.earth.28.1.611

Li, G. J., Chen, J., Ji, J. F., Yang, J. D., and Conway, T. M. (2009). Natural and anthropogenic sources of East Asian dust. *Geology*, **37**(8)*,* 727-730. https://doi.org/10.1130/G30031A.1

Liu, C. C., and Deng, C. L. (2012a). Magnetic mineralogy of the red soil sequences in southern China and its variety. *Quaternary Science*, **32**(4), 626-634. https://doi.org/10.3969/j.issn.1001-7410.2012.04.07

Liu, Q. S., Bloemendal, J., Torrent, J., and Deng, C. L. (2006). Contrasting behavior of hematite and goethite within paleosol S5 of the Luochuan profile, Chinese Loess Plateau. *Geophysical Research Letters*, **33**(20), L20301. https://doi.org/10.1029/2006GL027172

Liu, Q. S., Deng, C. L., Torrent, J., and Zhu, R. X. (2007a). Review of recent developments in mineral magnetism of the Chinese loess. *Quaternary Science Reviews*, **26**(3-4), 368-385. https://doi.org/10.1016/j.quascirev.2006.08.004

Liu, Q. S., Roberts, A. P., Torrent, J., Horng, C. S., and Larrasoaña, J. (2007b). What do the HIRM and *S-ratio* really measure in environmental magnetism? *Geochemistry Geophysics Geosystems*, **8**(9), Q09011. https://doi.org/10.1029/2007GC001717

Liu, T. S., and Ding, Z. L. (2003). Chinese loess and paleomonsoon. *Annual Review of Earth and Planetary Sciences*, **26**(1), 111-145. https://doi.org/10.1146/annurev.earth.26.1.111

Liu, T. S. (1985). Loess and environment. (p.16-17). Beijing: Science Press

Liu, X. M., Rolph, T., Bloemendal, J., Shaw, J., and Liu, T. S. (1995). Quantitative estimates of palaeoprecipitation at Xifeng, in the Loess Plateau of China. *Palaeogeography, Palaeoclimatology, Palaeoecology*, **113**(2-4), 243-248. https://doi.org/10.1016/0031-0182(95)00053-o

Liu, X. M., Hesse, P., Begét, J., and Rolph, T. (2001). Pedogenic destruction of ferrimagneticsin Alaskan loess deposits. *Australian Journal of Soil Research*, **39**(1), 99-115. https://doi.org/10.1071/SR99081

Liu, X. M., Rolph, T., An, Z., and Hesse, P. (2003). Paleoclimatic significance of magnetic properties on the Red Clay underlying the loess and paleosols in China. *Palaeogeography, Palaeoclimatology, Palaeoecology*, **199**(1-2), 153-166. https://doi.org/10.1016/S0031-0182(03)00504-2

Liu, X. M., Liu, Z., Lü, B., Markovic, S. B., Chen, J. S., Guo, H., Ma, M., Zhao, G. Y., and Feng, H. (2012b). The magnetic properties of Serbian loess and its environmental significance. *Chinese Science Bulletin*, **57**(33), 3173-3184. https://doi.org/10.1007/s11434-012-5383-9

Long, X. Y., Ji, J. F., and Balsam, W. (2011). Rainfall-dependent transformations of iron oxides in a tropical saprolite transect of Hainan Island, South China: Spectral and magnetic measurements. *Journal of Geophysical Research-Earth Surface*, **116**, F03015. https://doi.org/10.1029/2010jf001712

Long, X. Y., Ji, J. F., Balsam, W., Barrón, V., and Torrent, J. (2015). Grain growth and transformation of pedogenic magnetic particles in red Ferralsols. *Geophysical Research Letters*, **42**(14), 5762-5770. https://doi.org/10.1002/2015gl064678

Long, X. Y., Ji, J.F., Barrón, V., and Torrent, J. (2016). Climatic thresholds for pedogenic iron oxides under aerobic conditions: Processes and their significance in paleoclimate reconstruction. *Quaternary Science Reviews*, **150**, 264-277. https://doi.org/10.1016/j.quascirev.2016.08.031

Lu, H. Y., Stevens, T., Yi, S. W., and Sun, X. F. (2006). An erosional hiatus in Chinese loess sequences revealed by closely spaced optical dating. *Chinese Science Bulletin*, **51**, 2253–2259. https://doi.org/10.1007/s11434-006-2097-x

Luo, Z., Nie, J. S, Moe, A., Heermance, R., Garzione, C., Herbert, T., Zhao, W., Li, H., Zhang, R., Zhao, X. M., and Salzmann, U. (2020). Joint insolation and ice sheet/CO2 forcing on northern China precipitation during Pliocene warmth. *Science Bulletin*, **66**(4), 319-322. https://doi.org/10.1016/j.scib.2020.10.025.

Maher, B. A. (1998). Magnetic properties of modern soils and Quaternary loessic paleosols, paleoclimatic implications. *Palaeogeography, Palaeoclimatology, Palaeoecology*, **137**(1-2), 25–54. https://doi.org/10.1016/S0031-0182(97)00103-X

Maher, B. A. (2016). Palaeoclimatic records of the loess/palaeosol sequences of the Chinese loess plateau. *Quaternary Science Reviews*, **154**, 23-84. https://doi.org/10.1016/j.quascirev.2016.08.004

Mehra, O. P., and Jackson, M. L. (1958). Iron oxide removal from soils and clays by a dithionite-citrate system buffered with sodium bicarbonate. *Clays and Clay Minerals,* **7**(1), 317-327. https://doi.org/10.1346/ccmn.1958.0070122

Molnar, P., and Tapponnier, P. (1975). Cenozoic Tectonics of Asia: Effects of a Continental Collision: Features of recent continental tectonics in Asia can be interpreted as results of the India-Eurasia collision. *Science, New Series*, **189**(4201), 419-426. https://doi.org/10.1126/science.189.4201.419

Mullins, C. E. (1977). Magnetic susceptibility of the soil and its significance in soil science: a review. *Journal of Soil Science*, **28**(2), 223-246. https://doi.org/ 10.1111/j.1365-2389.1977.tb02232.x

Navrotsky, A., Mazeina, L., and Majzlan, J. (2008). Size-driven structural and thermodynamic Complexity in Iron Oxides. *Science (New York, N.Y.)*, **319**(5870), 1635-1638. https://doi,org/10.1126/science.1148614.

Nie, J. S., King, J. W., and Fang, X. M. (2008). Link between benthic oxygen isotopes and magnetic susceptibility in the red-clay sequence on the Chinese loess plateau. *Geophysical Research Letters*, **35**(3), L03703. http://doi.org/10.1029/2007GL032817

Nie, J. S., Song, Y. G., King, J. W., Fang, X. M., and Heil, C. (2010). HIRM variations in the Chinese red-clay sequence: insights into pedogenesis in the dust source area. *Journal of Asian Earth Sciences*, **38**(3-4), 96-104. https://doi.org/10.1016/j.jseaes.2009.11.002Get rights and content

Nie, J. S., Song, Y. G., King, J., and Zhang, R. (2013). Six million years of magnetic grain-size records reveal that temperature and precipitation were decoupled on the Chinese Loess Plateau during 4.5–2.6 Ma. *Quaternary Research*, **79**(3), 465–470. https://doi.org/10.1016/j.yqres.2013.01.002

Nie, J. S., Stevens, T., Song, Y. G., King, J. W., Zhang, R., Ji, S. C., Gong, L. S., and Cares, D. S. (2014). Pacific freshening drives Pliocene cooling and Asian monsoon intensification. *Scientific Reports*, **4**(1), 5474. https://doi.org/10.1038/srep05474

Nie, J. S., Garzione, C., Su, Q. D., Liu, Q. S., Zhang, R., Heslop, D., Cristian, N., Zhang, S. H., Song, Y. G., and Luo, Z. (2017). Dominant 100,000-year precipitation cyclicity in a late Miocene lake from Northeast Tibet. *Science Advances*, **3**(3), e1600762. https://doi.org/10.1126/sciadv.1600762

Pelxoto, J., and Oort, A. H. (1996). The Climatology of Relative Humidity in the Atmosphere. *Journal of Climate,* **9**(12), 3443-3463. https://doi.org/ 10.1175/1520-0442(1996)0092.0.CO;2

Ren, J., Long, X. Y., Ji, J. F., Barrón, V., Torrent, J., Wang, Y., and Xie, S. Y. (2020). Different enrichment patterns of pedogenic magnetic particles modulated by primary iron-phosphorous input. *Geophysical Research Letters*, **47**(22), e2020GL 090439. https://doi.org/10.1002/essoar.10503638.1.

Schwertmann, U. (1964). Differenzierung der Eisenoxide des Bodens durch Extraktion mit Ammoniumoxalat-Löesung. *Journal of Plant Nutrition and Soil Science*, **105** (3), 194-202. https://doi.org/10.1002/jpln.3591050303

Schwertmann, U. (1971). Transformation of hematite to goethite in soils. *Nature*, **232**(53113), 624-625. https://doi.org/10.1038/232624a0

Schwertmann, U. (1985). The effect of pedogenic environments on iron oxide minerals. *Advances in Soil Science*, **1**, 107-200. https://doi.org/10.1007/978-1-4612-5046-35

Tardy, Y., and Nahon, D. (1985). Geochemistry of laterites, stability of Al-goethite, Al-hematite, and Fe^{3+}-kaolinite in bauxites and ferricretes; an approach to the mechanism of concretion formation. *American Journal of Science*, **285**(10), 865-903. https://doi.org/10.2475/ajs.285.10.865

Thompson, R., and Oldfield, F. (1986). Environmental Magnetism. (p.227). London: Allen &Unwin. https://doi.org/10.1007/978-94-011-8036-8

Torrent, J., Guzman, R., and Parra, M. (1982). Influence of relative humidity on the crystallization of Fe (III) oxides from ferrihydrite. *Clays Clay Miner*. **30** (5), 337-340. https://doi.org/10.1346/CCMN.1982.0300503

Torrent, J., Barrón V., and Liu, Q. (2006). Magnetic enhancement is linked to and precedes hematite formation in aerobic soil. *Geophysical Research Letters*, **33**, L02401. https://doi.org/10.1029/ 2005GL024818.

Torrent, J., Liu, Q. S., Bloemendal, J., and Barrón, V. (2007). Magnetic enhancement and iron oxides in the upper Luochuan loess-paleosol sequence, Chinese loess Plateau. *Soil Science Society of America Journal*, **71**(5), 1570-1578. https://doi.org/ 10.2136/sssaj2006.0328

Trolard, F., and Tardy, Y. (1987). The stabilities of gibbsite, boehmite, aluminous goethites and aluminous hematites in bauxites, ferricretes and laterites as a function of water activity, temperature and particle size. *Geochimica et Cosmochimica Acta*, **51**(4), 945-957. https://doi.org/10.1016/0016-7037(87)90 107-4

White, A. F., and Blum, A. E. (1995). Effects of climate on chemical weathering in watersheds. *Geochimica et Cosmochimica Acta,* **59**(9), 1729-1747. https://doi.org/10.1016/0016-7037(95)00078-E

Worm, H. U. (1998). On the superparamagnetic stable single domain transition for magnetite, and frequency dependence of susceptibility. *Geophysical Journal International*, **133**(1), 201-206. https://doi.org/10.1046/j.1365-246X.1998.1331468.x

Worm, H. U., and M. Jackson (1999). The superparamagnetism of Yucca Mountain Tuff. *Journal of Geophysical Research Solid Earth*, **104**(B11), 25415-25425. https://doi.org/10.1029/1999JB900285

Xie, Y. Y., Li, C. A.,Chang, X. Q. and Zhou, J. (2003). Climatic evolution of loess on the northeastern margin of the Qinghai-Tibet Plateau and its coupling with plateau uplift. *Geology in China*, **30**(4), 436-441. https://doi.org/10.3969/j.issn.1000-3657.2003.04.019

Xu, Y. H. (1991). Southwest Climate, China. (p.161). Beijing: China Meteorological Press.

Yang, D. Y., Li, L. P., Huang D., Ge, Z. S., Xu, Q. M., Li, X. S., and Han, Z. Y. (2010). Uplift characteristics of the Yunnan Plateau. *Quaternary Science*, **30***(5)*, 864-871. https://doi.org/10.3969/j.issn.1001-7410.2010.05.02

Yan, P., Yang, N., and Ye, B. Y. (2011). The extraction and study of geomorphic surface in Guizhou and its adjacent areas based on ASTER-GDEM. *Remote Sensing for Land and Resources*, **23**(2), 98-103. https://doi.org/10.3724/SP.J.1011.2011.00403

Yang, S. L., Fang, X. M., Li, J., An, Z. S., and Hitoshi, F. (2001). Transformation functions of soil color and climate. *Science in China Series D Earth Science,* **44**, 218–226. https://doi.org/10.1007/BF02911990

Yang, S. L., and Ding, Z. L. (2003). Color reflectance of Chinese loess and its implications for climate gradient changes during the last two glacial-interglacial cycles. *Geophysical Research Letters*, **30**(20), 2058. https://doi .org/10.1029/2003 GL018346.

Zhao, J., Fang, X. Q., and Wang, W. (2015). New Physical geography of China. (p.1-464). Beijing: High Education Press.